

Silicate mineralogy in the later fractionation stages of the Inch intrusion, NE Scotland

W. J. WADSWORTH

Department of Geology, The University, Manchester M13 9PL

ABSTRACT. Despite poor exposures and lack of 'stratigraphic' control, there is consistent mineralogical and textural evidence that the Inch Upper Zone (UZ) represents a cumulate sequence developed from a single episode of progressive fractionation. This sequence has been subdivided on the basis of the phase layering, with cumulus plagioclase, pyroxenes and Fe-Ti oxides providing continuity from the Middle Zone (although the pyroxenes appear to be temporarily restricted to inter-cumulus status in the lower part of the UZ succession). The reappearance of cumulus olivine after its absence throughout the Middle Zone, marks the base of the UZ, and it is later joined by cumulus apatite, and then by alkali feldspar and zircon. Higher in the succession cumulus orthopyroxene, followed by olivine and Fe-Ti oxide, eventually disappear. There is pronounced cryptic variation of the principal cumulus minerals (olivine $Fo_{4.7-6}$, orthopyroxene En_{58-24} , clinopyroxene $Mg\#_{6.3-6}$, plagioclase An_{60-39}) and the cumulus alkali feldspar is distinctly Ba-rich when it first appears. Comparison with the later fractionation stages of other layered intrusions shows broad similarities to the Bushveld and Skaergaard intrusions and closer similarities to the Fongen-Hyllingen body, which, like Inch, is a Caledonian synorogenic intrusion. The behaviour of the Inch pyroxenes, which show smoothly progressive Fe-enrichment despite their temporary absence as cumulus phases early in the UZ, together with the apparent range in cumulus plagioclase compositions in each sample, are taken to indicate that the cumulus mineral assemblages have been to some extent modified by re-equilibration with trapped inter-cumulus magma.

KEYWORDS: Silicate minerals, cumulate sequence, Inch intrusion, Scotland.

THE Inch intrusion is not only the largest of the Caledonian Newer Gabbro bodies in NE Scotland, but also comprises the greatest variety of rock types (Wadsworth, 1982). The most distinctive component, and one which is hardly represented among the other Newer Gabbro intrusions, is a series of ferrogabbros and ferrodiorites, grading into ferrosyenodiorites and quartz-syenites. The first modern account of these rocks was given by Read *et al.* (1961), who grouped them together as the 'Inch Differentiated Suite' and regarded them as comple-

mentary to the 'Bourtie Dunite-Troctolite Series' (occurring at the eastern end of the Inch mass), in representing the fractionation products of a parental gabbroic magma.

Subsequent studies of the Inch intrusion by Clarke and Wadsworth (1970) led to the recognition of a relatively complete cumulate sequence, divided into three principal stratigraphic units. These were termed Lower Zone (equivalent to the 'Bourtie Dunite-Troctolite Series'), Middle Zone (consisting of hyperthene-gabbros, previously interpreted by Read *et al.* (1965) as resulting from contamination of the regional gabbroic magma), and Upper Zone (equivalent to the 'Inch Differentiated Suite') respectively. The Upper Zone (UZ) was further divided into three sub-units (UZa, UZb, UZc) based on stratigraphic variations of the cumulus mineral assemblage, especially with respect to olivine, orthopyroxene, and alkali feldspar. In addition, Clarke and Wadsworth (1970) were able to demonstrate systematic variations in the cumulus mineral compositions, particularly within the UZ, although it should be emphasized that their results were based mainly on optical determinations (olivine, orthopyroxene, and plagioclase), with supplementary information from chemical analysis of separated minerals (clinopyroxene and alkali feldspar). In summary, the following approximate composition ranges from bottom to top of the UZ were indicated: olivine (Fo_{40} to Fo_5), orthopyroxene (En_{45} to En_{25}), clinopyroxene ($Ca_{35}Mg_{35}Fe_{30}$ to $Ca_{40}Mg_5Fe_{55}$), and plagioclase (An_{55} to An_{40}). It was also noted that cumulus alkali feldspar varied from Ba-rich, when it first appeared as a cumulus phase at the base of UZb, to Ba-poor in the most evolved member of UZc. Read *et al.* (1961) had already hinted at significant Ba contents in the alkali feldspars and micas, on the basis of whole-rock chemical analyses.

The present study represents a further stage in characterizing the variations in mineral composition within the Inch Upper Zone, and is based essentially on electron microprobe analyses of all

the main silicate phases in fourteen rocks, covering the full range of UZ compositions. It is part of a wider mineralogical and geochemical re-investigation of the Inch intrusion and comparison with neighbouring Newer Gabbro bodies.

Field relations

Upper Zone rocks occur in a NE-SW trending belt (up to 5 km in width) in the central region of the Inch intrusion, with the town of Inch at the approximate mid-point of the southern edge of this belt (fig. 1). Exposure is generally rather poor, although better than in either the Middle or Lower Zones of the intrusion. The scarce natural outcrops are supplemented by artificial exposures in a number of small quarries, but unfortunately many of these have been filled in during the past twenty years. However, recent excavation of a gas pipeline trench, has provided valuable temporary exposures in a NW-SE traverse across the central part of the intrusion (fig. 1). The UZ rocks characteristically

exhibit prominent spheroidal weathering, with the result that extremely fresh material is often available as residual kernels, even in the most unpromising exposures.

The main problem in establishing the precise fractionation sequence of the Inch UZ is the lack of stratigraphic control. The broad compositional variations, with the MZ rocks occurring generally to the SE of the UZ area (and the LZ rocks further to the east) and the most evolved members (UZc) capping the series of small hills (the 'Red Rock Hills' of Read *et al.*, 1961) running NE-SW through the middle of the UZ belt (see fig. 1), suggest that the UZ rocks dip gently NW in the vicinity of their contact with the MZ, and become approximately horizontal in the central part of the area. Much of this interpretation is based on the assumption that the Inch rocks represent a cumulate succession (or at least that their differentiation was gravity-controlled and resulted in an ordered 'stratigraphic' sequence of progressively more evolved compositions). Unfortunately there is no direct evidence of

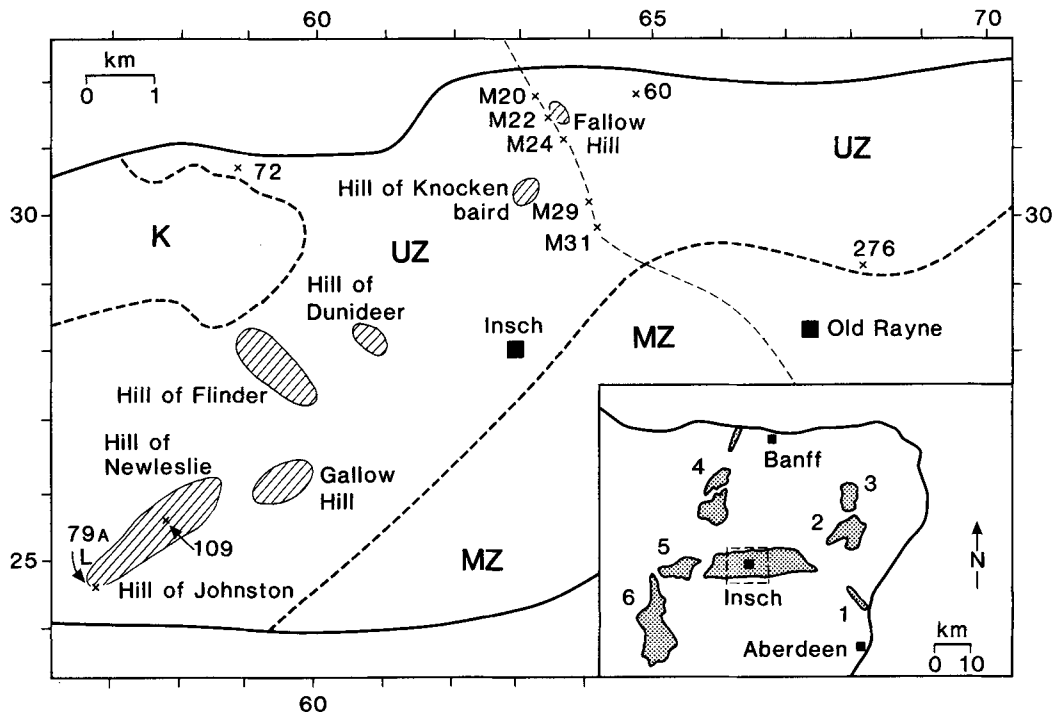


FIG. 1. Geological sketch map of the central part of the Inch intrusion, showing the distribution of the Upper Zone (UZ) in relation to the Middle Zone (MZ) and the Kennethmont Granite-Diorite Complex (K). The areas in which UZb and UZc rocks occur (Red Rock Hills) are indicated by diagonal ornament. *In situ* specimen localities are also shown (X), and the position of the gas pipeline is marked by the fine dashed line. The grid references relate to National Grid Square NJ. The inset map relates the Inch intrusion to the other Caledonian Newer Gabbros (1, Belhelvie; 2, Haddo-Arnage; 3, Maud; 4, Huntly; 5, Bogancloch; 6, Morven-Cabrach).

small-scale layering within the UZ to confirm this interpretation, and the textural evidence that these rocks are cumulates is hardly compelling, although this is not surprising in view of the number of potential cumulus minerals involved. However, there is little doubt that the overall variation represented by the sequence UZa → UZb → UZc is broadly 'stratigraphic', as well as evolutionary in the petrogenetic sense, but the combination of limited exposure, gentle topography, and quasi-horizontal attitude, make it impossible to relate individual rock samples to an established stratigraphic framework, such as is the case with most layered intrusions. For the same reasons, any estimates of stratigraphic thickness of the UZ as a whole (or its component subzones) such as those proposed by Clarke and Wadsworth (1970), must be taken as approximations at best.

In practice, the only effective way to proceed was to assume that the UZ rocks represented a simple fractionation series and to use the mineral compositions rather than the field relationships, to establish

the precise sequence, unless it became apparent that the situation was more complicated. In the event, a preliminary reconnaissance of the mineral compositions revealed a straightforward pattern of variation, consistent with a single progressive fractionation event, and without any major anomalies in terms of geographical distribution. As far as possible, only *in situ* material was used, but the reconnaissance involved analyses from a total of thirty-five samples, of which twelve were not from genuine exposures. From this collection, a representative set of fourteen rocks was selected to cover the compositional range established in the initial reconnaissance. Of these, only three were not collected *in situ*, and these were incorporated either because they extended the apparent range (NL2) or conveniently filled a gap in the sequence (GL2 and N). The main (*in situ*) sample localities are shown in fig. 1 and their grid references are given in Table I. It should be noted that five of the samples (those with an M prefix) come from a 2 km stretch of the gas pipeline trench, but even here the geographical and

Table I Summary of Insch Upper Zone (UZ) mineralogy

	Olivine		Orthopyroxene			Clinopyroxene			Plagioclase		Alkali Feldspar			Amphibole		Biotite	Apatite	Zircon	Opaques
	Fo	En	Ca	Mg	Fe	An	Ab	Or	Cn	Mg*	Mg*								
109	-	-	44.9	3.3	51.9	38.7	18.0	81.3	0.7	-	-	-	-	-	-	-	-	c	-
M22	-	-	45.5	5.3	49.2	39.6	18.6	78.7	2.7	-	-	-	-	-	-	-	-	c	-
L	5.5	-	45.0	12.0	43.0	40.9	18.6	76.4	5.0	(16.6)	(18.1)	c	c	c	-	-	-	c	-
79A	9.5	23.9	44.4	19.3	36.4	44.2	19.2	70.8	10.0	(23.3)	(23.0)	c	c	c	-	-	-	c	-
M24	13.5	29.3	43.9	22.5	33.6	48.8	19.1	67.9	13.0	(n.a.)	(n.a.)	c	c	c	-	-	-	c	c
72	18.2	33.9	43.3	25.8	30.9	52.4	-	-	-	(31.4)	(31.0)	c	-	-	-	-	-	c	-
M20	25.9	41.1	43.7	29.3	27.0	54.0	-	-	-	(n.a.)	(n.a.)	c	-	-	-	-	-	c	-
N	28.5	44.4	44.2	30.0	25.8	53.1	-	-	-	(42.4)	(40.9)	c	-	-	-	-	-	c	-
60	31.5	(47.6*)	(45.2	30.7	24.1)	55.1	-	-	-	-	(n.a.)	c	-	-	-	-	-	c	-
M31	33.4	(48.5*)	(44.5	31.6	23.9)	55.7	-	-	-	-	(n.a.)	-	-	-	-	-	-	c	-
M29	36.6	(49.7*)	(45.6	32.1	22.3)	56.8	-	-	-	-	(51.0)	-	-	-	-	-	-	c	-
GL2	39.9	(51.6*)	(45.1	33.0	21.9)	57.6	-	-	-	(n.a.)	(n.a.)	-	-	-	-	-	-	c	-
276	42.4	(54.7)	-	-	-	58.0	-	-	-	-	(n.a.)	c	-	-	-	-	-	c	-
NL2	46.7	58.0	(44.9	34.7	20.4)	59.8	-	-	-	(52.9)	(58.0)	-	-	-	-	-	-	c	-

Mg* = 100 x Mg/(Mg + Fe) c = cumulus phase (in the case of non-silicates) * inverted pigeonite n.a. = not analysed
Compositions refer to probable cumulus phases (except those in brackets which appear to be of intercumulus habit).

Specimen Localities (grid reference in brackets)

109	(580 256)	Hill of Newieslie	N	(652 297)	Little Ledikin (not in situ)
M22	(637 315)		60	(649 319)	Williamston House
L	(570 247)	Bridge of Johnston	M31	(644 299)	
79A	(570 247)	Bridge of Johnston	M29	(643 304)	
M24	(638 312)		GL2	(723 269)	Glenlogie (not in situ)
72	(589 308)	Brankston	276	(683 293)	Mill of Bonnyton
M20	(634 318)		NL2	(696 291)	Newlands (not in situ)

M prefixes refer to material from the temporary gas pipe-line trench N.E. of Insch (see Fig. 1).

stratigraphical relationships are complicated by the fact that the trench apparently progresses from UZa to UZc, and then back to UZa as it cuts from NW to SE through the flanks of one of the 'Red Rock Hills' (Fallow Hill). The only place where the field relations are clear-cut is in the small quarry at the foot of Hill of Johnston, where L was collected a few metres above 79A. Despite the well-established succession and relatively good exposures on these 'Red Rock Hills', the rocks are almost always heavily weathered, and it is impossible to collect a full range of sufficiently fresh UZb and UZc material from a single locality, where there would be obvious advantages from the stratigraphical point of view. However, it is hoped that drill core recently made available (by courtesy of Dr M. Munro of Aberdeen University) from Gallow Hill, WSW of Inch town, may be used to establish the precise stratigraphic sequence of variations occurring in the final stages of differentiation.

Mineralogy

The principal mineralogical variations within the Inch Upper Zone are summarized in Table I and fig. 6, both in terms of mineral assemblage and mineral composition, for the fourteen rocks forming the type succession. The base of UZa is defined by the reappearance of cumulus* olivine after its absence throughout the MZ. The MZ rocks are characterized by the cumulus assemblage of clinopyroxene, orthopyroxene, plagioclase, and Fe-Ti oxide, and these phases occur throughout UZa. However, it should be noted that the pyroxenes (especially clinopyroxene) tend to be relatively scarce in the lower part of UZa, and are typically of intercumulus habit, suggesting that there may not be a simple evolutionary relationship between MZ and UZ. (Preliminary investigation of the mineral compositions in the MZ rocks confirms this.) Apatite first appears as a cumulus phase within UZa (and not within the MZ, as stated by Clarke and Wadsworth, 1970). It occurs sporadically in the lower part of the subzone but only becomes firmly

* The term 'cumulus' is used here in the sense proposed by Irvine (1982) to describe early crystallizing components of the rocks (as indicated by textural criteria), without necessarily implying that crystal settling of these components has occurred. However, the fact that such rocks are generally part of a broad evolutionary sequence, indicates the operation of a continuous differentiation mechanism. It is considered inherently likely that such differentiation involved fractional crystallization (rather than any pre-crystallization liquid differentiation), and that the actual mechanism was gravity-controlled, involving preferential segregation of cumulus crystals from the associated liquid phase.

established at a higher level, at approximately the same stage as the pyroxenes achieve definite cumulus status. Intercumulus biotite occurs in most of the UZa rocks, and intercumulus amphibole is sometimes present as well.

The base of UZb is characterized by the appearance of cumulus alkali feldspar and zircon, as proposed by Clarke and Wadsworth (1970). This means that many UZb rocks contain as many as eight cumulus phases (olivine, orthopyroxene, clinopyroxene, plagioclase, alkali feldspar, apatite, zircon, and Fe-Ti oxide). However, it appears that cumulus orthopyroxene does not persist to the top of this subzone. Intercumulus amphibole and biotite are generally present, while small amounts of quartz occur locally.

UZc is distinguished by the final disappearance of cumulus olivine, apatite and Fe-Ti oxide, so that the rocks of this subzone consist essentially of abundant alkali feldspar, together with plagioclase, clinopyroxene and minor zircon. It is not clear whether these are genuine cumulus phases, or whether UZc is equivalent to the Sandwich Horizon in the Skaergaard intrusion (Wager and Brown, 1968), perhaps representing *in situ* crystallization of the final residual magma. Amphibole and biotite are generally scarce in UZc, except as alteration products of the ferromagnesian constituents, but interstitial quartz occurs locally.

It is apparent that a more complete record of cumulus mineral behaviour (especially the pyroxenes and apatite) would permit further subdivision of the Inch Upper Zone. However, for the moment, it is considered expedient to retain the threefold division introduced by Clarke and Wadsworth (1970).

Microprobe analyses (energy-dispersive mode only) were undertaken on all the silicate minerals occurring as cumulus phases (except zircon), and in each case between 5 and 15 spots, restricted to the crystal cores or apparent cores, were analysed (see appendix for analytical conditions). The intercumulus pyroxenes in the lower part of UZa have all been analysed, again avoiding the more obviously marginal areas of the crystals, but intercumulus amphibole and biotite have only been studied at selected points in the sequence. It is intended to investigate the compositional variations in the non-silicates (apatite and Fe-Ti oxides) at a later stage.

Olivines (Table II). Cumulus olivine is consistently present throughout UZa and UZb, and shows progressive Fe-enrichment from Fo₄₇ to Fo₆. Mn shows a sympathetic increase (0.015–0.058 cations per formula unit, equivalent to a variation in mol. % tephroite from 0.7 to 2.9), but Ca and Ni are below detection limits for EDS analyses. The extent of the

THE INSCH INTRUSION

587

Table II Representative analyses of olivines

	NL2	276	GL2	M29	M31	60	N	M20	72	M24	79A	L
SiO ₂	34.75	34.19	33.78	33.28	33.31	31.97	32.58	31.93	31.20	30.10	29.95	29.60
FeO†	43.75	46.68	48.35	50.09	50.99	52.86	54.74	56.03	59.89	62.12	63.94	66.82
MnO	0.61	0.56	0.71	0.72	1.02	0.85	0.88	0.87	1.33	1.71	1.74	2.05
MgO	21.55	19.29	18.01	16.32	14.37	13.66	12.23	10.96	7.48	5.46	3.77	2.18
Total	100.66	100.72	100.85	100.41	99.69	99.34	100.43	99.79	99.90	99.39	99.40	100.65

Cations to 4 oxygens

Si	1.002	1.001	0.998	0.998	1.013	0.988	1.003	0.999	1.000	0.989	0.994	0.983
Fe	1.055	1.143	1.194	1.256	1.297	1.367	1.410	1.467	1.606	1.707	1.776	1.856
Mn	0.015	0.014	0.018	0.018	0.026	0.022	0.023	0.023	0.036	0.048	0.049	0.058
Mg	0.926	0.842	0.793	0.730	0.651	0.629	0.561	0.512	0.357	0.267	0.187	0.108
Fe	46.7	42.4	39.9	36.8	33.4	31.5	28.5	25.9	18.2	13.5	9.5	5.5

† Total Fe as FeO (Ca and Ni below detection limits by EDS)

Table III Representative analyses of orthopyroxenes

	NL2	276	GL2*	M29*	M31*	60*	N	M20	72	M24	79A
SiO ₂	51.72	51.43	51.22	51.13	51.02	50.16	50.28	49.46	48.83	48.30	47.95
TiO ₂	0.19	-	0.26	0.29	-	0.25	0.18	-	0.21	-	-
Al ₂ O ₃	1.22	1.18	1.03	1.12	0.87	1.13	0.77	0.79	0.40	0.68	0.43
FeO†	25.31	26.88	28.73	29.67	30.39	30.55	32.30	34.05	36.73	39.00	41.31
MnO	0.58	0.59	0.82	0.67	0.83	0.67	0.75	0.78	1.10	1.25	1.57
MgO	19.61	18.22	17.18	16.48	16.10	15.59	14.46	13.31	10.56	9.09	7.26
CaO	1.36	0.99	1.24	1.24	1.32	1.29	1.23	1.13	1.57	1.33	1.11
Total	99.99	99.29	100.48	100.60	100.33	99.64	99.97	99.52	99.40	99.65	99.63

Cations to 6 oxygens

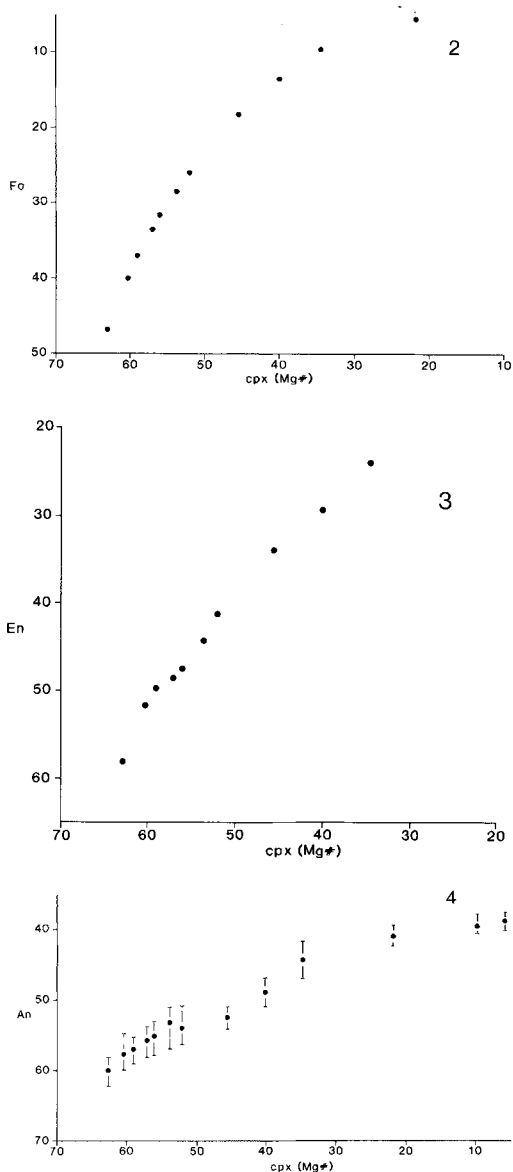
Si	1.961	1.976	1.966	1.967	1.978	1.962	1.976	1.972	1.983	1.979	1.983
Ti	0.005	0.000	0.007	0.008	0.000	0.007	0.005	0.000	0.006	0.000	0.000
Al	0.055	0.053	0.047	0.051	0.031	0.052	0.036	0.037	0.019	0.033	0.021
Fe	0.803	0.864	0.922	0.955	0.986	0.999	1.061	1.135	1.247	1.336	1.428
Mn	0.019	0.019	0.027	0.022	0.027	0.022	0.025	0.026	0.038	0.043	0.055
Mg	1.109	1.044	0.983	0.945	0.930	0.909	0.847	0.791	0.639	0.555	0.448
Ca	0.055	0.041	0.051	0.051	0.055	0.054	0.052	0.048	0.068	0.058	0.049
Ca	2.8	2.1	2.6	2.6	2.8	2.8	2.7	2.4	3.5	3.0	2.5
Mg	56.4	53.6	50.3	48.4	47.2	46.3	43.2	40.1	32.7	28.5	23.3
Fe	40.8	44.3	47.1	49.0	50.0	50.9	54.1	57.5	63.8	68.5	74.2
En	58.0	54.7	51.6	49.7	48.5	47.6	44.4	41.1	33.9	29.3	23.9

† Total Fe as FeO * inverted pigeonite

olivine composition gap represented by the Insch Middle Zone is not precisely known. The most magnesian olivine so far recorded ($Fo_{46.7}$) in the UZ is from a loose boulder (NL2), and it is possible that slightly more magnesian compositions may be found in due course. Lack of exposure in the vicinity of the MZ/LZ boundary makes it more difficult to estimate the lower limit of the olivine composition gap. The least magnesian olivine so far recorded in undoubted LZ cumulates from the Insch intrusion is Fo_{75} (from exposures in a temporary trench near Mill of Bourtie). Olivines in the range Fo_{57-62} are found locally within the supposed MZ area, but these are texturally quite distinct from the typical MZ cumulates. They are probably related to the suite of granular hypersthene-gabbros described by Clarke and Wadsworth (1970) and interpreted by them as a separate intrusion. The Insch olivine gap is therefore provisionally recorded as Fo_{75} to Fo_{47} .

Orthopyroxenes (Table III). Orthopyroxene occurs throughout UZA and most of UZb. However, its range as a definite cumulus phase is apparently more restricted (to the base and upper part of UZA, and to UZb). In the lower middle part of UZA it forms distinctive poikilitic crystals of inverted pigeonite, with characteristically blebby exsolution of Ca-rich pyroxene. Despite this apparent change in status from cumulus to intercumulus and back to cumulus, the orthopyroxene shows progressive Fe-enrichment from En_{58} to En_{24} . There is a corresponding increase in Mn (0.019–0.055 cations per formula unit) and a slightly less regular decrease in Al (0.05–0.02 cations per formula unit). Ti is obviously close to detection limits using EDS, and the recorded variations are probably not significant. Ca is relatively constant (averaging 2.7% mol. % Wo), but it should be emphasized that the bulk Ca content of these pyroxenes must be slightly higher than recorded in Table III, especially for the inverted pigeonites, because the more obvious exsolution lamellae were avoided for the purposes of microprobe analysis. The cumulus orthopyroxenes typically show traces of fine exsolution lamellae of Ca-rich pyroxene parallel to (100), especially in UZA. All the UZ orthopyroxenes are pleochroic (pale pink to pale green) but the intensity of pleochroism decreases with progressive Fe (and Mn) enrichment.

Clinopyroxenes (Table IV). Ca-rich clinopyroxene is generally present throughout the complete UZ range. It is a relatively minor constituent in the lower part of UZA (and cannot be detected at all in 276), and is apparently of intercumulus habit in this part of the succession. However, as with orthopyroxene, it displays progressive Fe-enrichment, regardless of its cumulus or intercumulus status,



Figs. 2–4. Olivine (2), orthopyroxene (3), and plagioclase (4) compositions plotted against clinopyroxene compositions [$Mg\# = 100 \times Mg/(Mg + Fe)$]. The bar lines in fig. 4 indicate the range of apparent plagioclase core compositions in each sample.

from $Mg\#63$ to $Mg\#6$, while Mn shows a broadly corresponding increase (0.01–0.04 cations per formula unit). Al decreases from 0.1 to 0.05 cations per formula unit during fractionation, and there is evidence of a Ca-minimum towards the top of UZA and into UZb (see fig. 5). Ti is low (generally just

Table IV Representative analyses of clinopyroxenes

	NL2	GL2	M29	M31	60	N	M20	72	M24	79A	L	M22	109
SiO ₂	51.31	51.41	51.81	51.12	50.93	50.84	51.36	50.73	49.14	48.92	48.29	46.80	46.75
TiO ₂	0.48	0.44	0.61	0.58	0.27	0.58	-	-	0.67	0.52	0.44	0.62	0.60
Al ₂ O ₃	2.15	2.31	1.68	1.90	1.58	1.85	0.79	0.97	1.55	1.45	1.23	1.41	1.04
FeO†	12.44	13.38	13.56	14.61	14.75	15.54	16.42	18.93	19.74	21.67	24.91	28.29	29.39
MnO	0.30	0.27	0.36	0.36	0.40	0.47	0.43	0.39	0.60	0.75	0.72	0.59	1.09
MgO	11.81	11.35	10.96	10.80	10.54	10.12	10.00	8.86	7.43	6.45	3.91	1.70	1.04
CaO	21.31	21.54	21.69	21.19	21.55	20.76	20.78	20.67	20.15	20.47	20.39	20.45	19.82
Na ₂ O	-	-	-	-	-	-	-	-	-	0.44	0.58	0.42	0.34
Total	99.80	100.70	100.67	100.56	100.02	100.16	99.78	100.55	99.28	100.67	100.47	100.28	100.07
Cations to 6 oxygens													
Si	1.939	1.940	1.958	1.944	1.952	1.949	1.978	1.963	1.943	1.932	1.943	1.923	1.936
Ti	0.014	0.013	0.017	0.017	0.008	0.017	0.000	0.000	0.020	0.015	0.013	0.019	0.019
Al	0.096	0.103	0.075	0.085	0.071	0.083	0.036	0.044	0.072	0.067	0.058	0.068	0.051
Fe	0.393	0.422	0.429	0.464	0.473	0.498	0.529	0.613	0.653	0.716	0.839	0.972	1.018
Mn	0.010	0.009	0.012	0.012	0.013	0.015	0.014	0.013	0.020	0.025	0.024	0.021	0.038
Mg	0.666	0.638	0.618	0.612	0.602	0.578	0.574	0.511	0.438	0.379	0.235	0.104	0.064
Ca	0.863	0.871	0.878	0.863	0.885	0.853	0.858	0.857	0.854	0.866	0.879	0.900	0.880
Na	0.000	0.000	0.000	0.000	0.000	0.000	0.000	0.000	0.000	0.034	0.045	0.033	0.027
Ca	44.9	45.1	45.6	44.5	45.2	44.2	43.7	43.3	43.9	44.4	45.0	45.5	44.9
Mg	34.7	33.0	32.1	31.6	30.7	30.0	29.3	25.8	22.5	19.3	12.0	5.3	3.3
Fe	20.4	21.9	22.3	23.9	24.1	25.8	27.0	30.9	33.6	36.4	43.0	49.2	51.9
Mg*	62.9	60.2	59.0	56.9	56.0	53.7	52.0	45.5	40.1	34.7	21.9	9.7	5.9

† Total Fe as FeO

Mg* = 100 x Mg/(Mg+Fe)

above detection limits) and shows no significant variation throughout the UZ. Na was only detected in clinopyroxenes from UZb and UZc. Fine exsolution lamellae of Ca-poor pyroxene occur parallel to (100) and (001) in clinopyroxenes from UZA, especially towards the top of this subzone, where they produce a strong schiller effect. In UZb and UZc the clinopyroxenes are characterized by two sets of opaque exsolution lamellae, which are assumed to be magnetite.

Plagioclases (Table V). Cumulus plagioclase occurs throughout the UZ, and is generally the most abundant cumulus phase, although it becomes subordinate to alkali feldspars in UZc. No individual analyses are presented because of the relatively wide range of compositions (generally between 4 and 6% An) resulting from microprobe analyses of plagioclase cores in individual rock samples. This feature seems to be typical of plagioclase in layered intrusions (see Wadsworth *et al.*, 1982, and Wadsworth, 1985). It appears to be much too patchy and unpredictable to be a growth (zoning) effect and is more likely to represent partial re-equilibration during the postcumulus stage of

crystallization. However, it is not immediately clear whether the average core composition (based on a minimum of eight microprobe analyses per rock, except in UZc) is more significant than the most calcic compositions, which may possibly represent remnants of the original cumulus material. Both are indicated in Table V and plotted in fig. 4, and together they demonstrate progressive fractionation throughout the UZ from An₆₀ to An₃₉ (using average core compositions), or from An₆₂ to An₄₀ (using the most calcic compositions recorded from each rock). The fact that there are slight discrepancies between adjacent samples in the sequence suggests that the number of analyses may still be insufficient. However, there is some evidence that the apparent composition range in individual rocks is less pronounced in UZc. Genuine marginal zoning also occurs in many cases, although usually on a minor scale, and this generally extends the compositions towards albite by a further 5%.

Alkali feldspars (Table VI). Cumulus alkali feldspar is present in UZb and UZc, becoming increasingly abundant (both in absolute terms and relative to plagioclase) with advancing fractionation. It is

Table V Summary of plagioclase core compositions

	NL2	276	GL2	M29	M31	60	N
Average	An 59.8	An 58.0	An 57.6	An 56.8	An 55.7	An 55.1	An 53.1
Range	58.4-62.2	56.3-59.2	54.8-59.8	55.4-58.9	53.8-58.0	53.2-57.9	51.0-57.0
Number of analyses	12	8	8	10	12	12	15
	M20	72	M24	79A	L	M22	109
Average	An 54.0	An 52.4	An 48.8	An 44.2	An 40.9	An 39.6	An 38.7
Range	50.9-56.3	51.1-53.9	46.9-50.9	41.6-46.9	39.5-42.1	37.9-40.6	37.4-40.0
Number of analyses	8	10	8	8	8	5	4

generally characterized by prominent microperthitic exsolution, but since the microprobe analyses were deliberately restricted to the more homogeneous areas, it is assumed that they represent the composition of the K-rich host crystal, rather than the bulk composition which must be more sodic. This is confirmed by a comparison of the microprobe data which show a composition range from $Or_{68}Ab_{19}An_0Cn_{13}$ to $Or_{81}Ab_{18}An_0Cn_{1}$, with partial analyses of mineral separates (reported by Clarke and Wadsworth, 1970, but adjusted to mol. %) which indicate a range from $Or_{63}Ab_{23}An_3Cn_{11}$ to $Or_{76}Ab_{22}An_1Cn_1$. The progressive reduction in Ba is clearly documented by the microprobe results. BaO decreases from 6.96 to 0.37 wt. %, corresponding to reduction in mol. % celsian from 13.0 to 0.7. There is optical evidence in 109 that the K-feldspar host is microcline, and this is also indicated by preliminary electron microscope (TEM) studies of the alkali feldspar in 79A. (Dr P. E. Champness, pers. comm.)

Amphiboles and biotites (Table VII). Intercumulus amphibole and biotite occur in many of the UZ rocks. Biotite in particular is found throughout UZa and UZb, and is always interstitial in habit, although it sometimes forms quite extensive poikilitic crystals. Amphibole only occurs sporadically in UZa, but is typically present in UZb. It is characteristically found in association with clinopyroxene, either as a marginal fringe, or as small 'inclusions' within the pyroxene. Microprobe analyses of amphibole and biotite were undertaken on selected samples to establish the range of compositions represented. There is clear evidence of pronounced Fe-enrichment through

the succession, in parallel with the cumulus ferromagnesian minerals (amphibole Mg# 52.9-16.6 and biotite Mg# 58.0-18.1). The amphiboles, which are essentially pargasitic hornblendes, show a corresponding increase in Mn and decrease in Ti, Al, Ca, and Na, although the trends are not

Table VI Representative analyses of alkali feldspars

	M24	79A	L	M22	109
SiO ₂	60.62	61.72	63.97	64.72	65.22
Al ₂ O ₃	19.70	19.50	18.77	18.68	18.79
BaO	6.96	5.28	2.78	1.47	0.37
Na ₂ O	2.05	2.06	2.08	2.10	2.04
K ₂ O	11.12	11.57	12.95	13.54	13.98
Total	100.45	100.13	100.55	100.51	100.40

Cations to 8 oxygens

Si	2.889	2.915	2.967	2.981	2.987
Al	1.106	1.086	1.026	1.014	1.014
Ba	0.130	0.098	0.050	0.027	0.007
Na	0.190	0.189	0.187	0.188	0.181
K	0.676	0.697	0.766	0.796	0.817
Ab	19.1	19.2	18.6	18.6	18.0
Or	67.9	70.8	76.4	78.7	81.3
Cn	13.0	10.0	5.0	2.7	0.7

Ca and Fe below detection limits (EDS)

Table VII Representative analyses of amphiboles and biotites

	NL2	N	72	79A	L	NL2	M29	N	72	79A	L
SiO ₂	41.62	42.06	42.60	41.44	41.03	36.31	35.79	34.98	34.83	34.27	34.19
TiO ₂	3.41	2.16	1.97	2.15	1.95	5.54	5.24	5.58	4.83	5.07	3.00
Al ₂ O ₃	12.38	11.35	9.37	9.56	9.41	15.24	15.00	14.48	14.54	13.98	13.93
FeO†	15.98	20.13	24.72	26.67	28.60	16.81	19.26	22.54	26.53	28.55	32.04
MnO	-	-	0.32	0.42	0.44	-	-	-	-	-	-
MgO	10.06	8.31	6.33	4.53	3.24	13.05	11.23	8.75	6.68	4.79	3.98
CaO	11.79	11.79	10.71	10.59	10.56	-	-	-	-	-	-
BaO	-	-	-	-	-	0.64	1.06	1.74	1.66	1.83	0.73
Na ₂ O	2.11	1.83	1.39	1.61	1.63	-	-	-	-	-	-
K ₂ O	1.21	1.06	0.87	1.18	1.20	9.49	9.08	8.68	8.61	8.35	8.37
Total	98.56	98.69	98.28	98.15	98.06	97.08	96.66	96.75	97.68	96.84	96.24

	Cations to 23 oxygens (amphiboles)					Cations to 22 oxygens (biotites)					
Si	6.214	6.376	6.312	6.524	6.221	5.408	5.429	5.417	5.438	5.466	5.536
Ti	0.383	0.246	0.219	0.255	0.222	0.621	0.598	0.650	0.567	0.608	0.365
Al	2.178	2.027	1.636	1.773	1.681	2.674	2.682	2.642	2.676	2.629	2.658
Fe	1.996	2.552	3.063	3.512	3.627	2.094	2.443	2.920	3.463	3.808	4.339
Mn	0.000	0.000	0.040	0.055	0.056	0.000	0.000	0.000	0.000	0.000	0.000
Mg	2.238	1.878	1.399	1.064	0.731	2.897	2.539	2.021	1.554	1.139	0.961
Ca	1.886	1.915	1.700	1.787	1.715	0.000	0.000	0.000	0.000	0.000	0.000
Ba	0.000	0.000	0.000	0.000	0.000	0.038	0.063	0.106	0.102	0.114	0.046
Na	0.609	0.536	0.399	0.490	0.479	0.000	0.000	0.000	0.000	0.000	0.000
K	0.231	0.205	0.164	0.237	0.232	1.804	1.756	1.715	1.716	1.699	1.728
Mg#	52.9	42.4	31.4	23.3	16.6	58.0	51.0	40.9	31.0	23.0	18.1

† Total Fe as FeO Mg# = 100 x Mg/(Mg+Fe)

smoothly progressive. The biotites have a significant Ba content which increases slightly throughout UZa, but is much reduced towards the end of UZb. This is consistent with the appearance of cumulus alkali feldspar at the beginning of UZb, causing progressive depletion of Ba in the magma, following a period of gradual Ba enrichment, which must have reached its peak at the end of UZa. The Ti content of the biotites is also considerably reduced at the same stage, having maintained a relatively constant level earlier in the succession.

Discussion

The mineralogical variations established in the preceding section clearly suggest that the Insch Upper Zone may be taken to represent a single progressive fractionation sequence. This is demonstrated by the relatively smooth curves resulting from plots of olivine, orthopyroxene and plagioclase compositions against Mg# [100 x Mg/(Mg + Fe)] of clinopyroxene (figs. 2-4), and by the simple tie-line relationships between co-existing clinopyroxene,

orthopyroxenes, and olivines (fig. 5). It may also be recalled that the initial reconnaissance involved microprobe analyses of cumulus minerals from an additional twenty-one samples, and all of

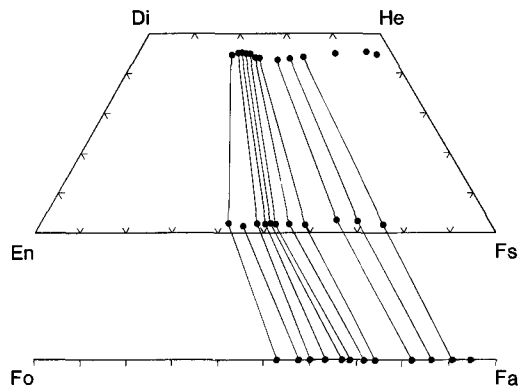


FIG. 5. Plot of coexisting clinopyroxene, orthopyroxene, and olivine compositions.

these fitted consistently into the overall pattern of mineralogical variation.

The lack of independent stratigraphic control means that the Insch UZ fractionation sequence cannot be firmly established as a layered succession, but mineralogical and textural comparisons with other, better exposed, layered intrusions makes it a reasonable inference. In particular, comparisons are made with the Skaergaard (Wager and Brown, 1968), Bushveld (Wager and Brown, 1968; Von Gruenewaldt, 1973) and Fongen-Hyllingen (Wilson *et al.*, 1981; Wilson and Larsen, 1985) intrusions, all of which are broadly similar to the Insch intrusion, consisting of upper zones in which cumulus olivine reappears after a significant period of absence in the middle part of the layered sequences. The overall pattern of phase layering and cryptic layering in the later evolutionary stages of all four intrusions is summarized in fig. 6.

Apart from the behaviour of cumulus olivine, the features common to these intrusions are the con-

tinuation of cumulus plagioclase, clinopyroxene and orthopyroxene from the olivine-free middle fractionation stages into the respective upper zones (although orthopyroxene, unlike clinopyroxene and plagioclase, fails to persist to the final stages, especially in the case of the Skaergaard intrusion where it disappears early in UZa), the appearance of cumulus apatite relatively soon after the re-appearance of olivine, and the occurrence of cumulus oxides (magnetite or magnetite plus ilmenite). These are generally already present before olivine reappears, but in the case of the Fongen-Hyllingen intrusion they enter the sequence just after olivine returns.

The similarities between the Insch and Fongen-Hyllingen intrusions are particularly marked (fig. 6). In both cases cumulus alkali feldspar and zircon make their appearance in the later stages of fractionation (after apatite), while orthopyroxene and olivine disappear successively just before the end of the sequence. The compositional ranges of the

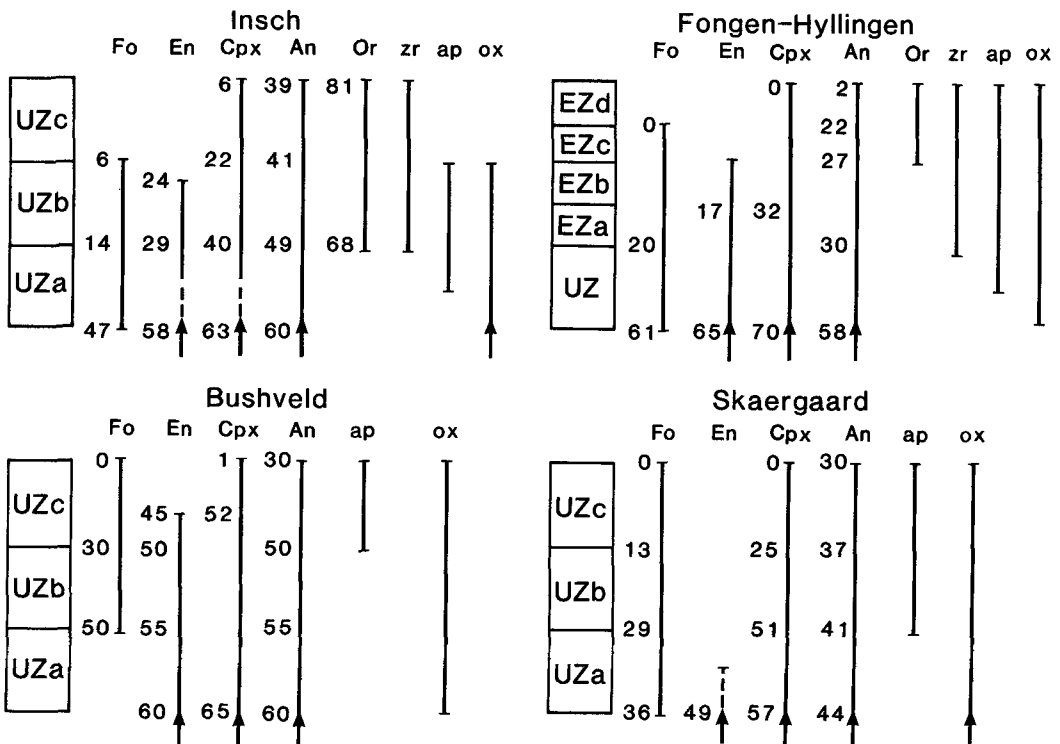


FIG. 6. Comparison of phase layering and cryptic layering patterns in the later fractionation stages of the Insch, Fongen-Hyllingen, Bushveld and Skaergaard intrusions (stratigraphic columns not to scale). Firm lines indicate cumulus ranges with arrows showing continuity from lower parts of the sequences. Dashed lines indicate intercumulus occurrences. Cpx compositions refer to $Mg\#[100 \times Mg/(Mg + Fe)]$; zr, ap, and ox refer to cumulus zircon, apatite, and Fe-Ti oxides respectively. EZ refers to the Extreme Zone of the Fongen-Hyllingen intrusion.

principal minerals are also reasonably similar except that the plagioclase at Fongen-Hyllingen reaches almost pure albite, compared with andesine (An_{39}) at Insch. Significant differences include the occurrence of cumulus amphibole, biotite, quartz and allanite in the Fongen-Hyllingen succession (none of these minerals achieves cumulus status at Insch), as well as the Ba-rich nature of the earliest cumulus alkali feldspar and the relatively early disappearance of cumulus apatite and Fe-Ti oxide at Insch. The combination of excellent exposure and the sequential appearance of a large number of cumulus phases in the later fractionation stages at Fongen-Hyllingen means that this part of the sequence has been more fully documented than in other intrusions, and is divided into two main units (Upper Zone followed by Extreme Zone), each of which is further subdivided (UZa to UZe, and EZa to EZd) on the basis of the phase layering (Wilson *et al.*, 1981). Further subdivision of the Insch succession along similar lines might be possible if more continuous exposure (or drill core) were available.

In addition to the mineralogical and petrological similarities between the Insch and Fongen-Hyllingen intrusions, it should also be emphasised that they occur in the same general geological setting. Both are essentially syntectonic within the Caledonian orogenic belt, although the Fongen-Hyllingen intrusion is distinctly younger (426 Ma compared with 480–500 Ma for Insch), and has been more substantially modified by associated regional metamorphic events.

No doubt, most of the differences in detail between these various layered intrusions reflect differences in parental magma compositions, and P - T conditions, which in turn have influenced the crystallization sequences developed during slow cooling. Of particular significance are the extent of the olivine composition gap and the composition range over which the orthopyroxene appears to be inverted pigeonite, but it is also of interest to compare the precise mineral compositions of the cumulus assemblages at specific stages in the evolutionary process, as marked by the principal phase changes.

The olivine composition gap at Insch is believed to be Fo_{75-47} , which compares with Fo_{71-61} at Fongen-Hyllingen (Wilson and Larsen, 1985), Fo_{53-36} at Skaergaard (Wager and Brown, 1968), and Fo_{85-50} at Bushveld (Wager and Brown, 1968). The cumulus mineral assemblages at the point when cumulus olivine reappears is seen to be $Fo_{47}/En_{58}/Mg\#(cpx)_{63}/An_{60}$ at Insch, $Fo_{61}/En_{65}/Mg\#(cpx)_{70}/An_{58}$ at Fongen-Hyllingen, $Fo_{36}/En_{49}/Mg\#(cpx)_{57}/An_{44}$ at Skaergaard, and approximately $Fo_{50}/En_{55}/Mg\#(cpx)_{60}/An_{55}$ at Bushveld.

Inverted pigeonite is restricted to the lower part of UZa at Insch, where it lies in the composition range En_{51-44} , and always occurs as extensive poikilitic crystals of presumed intercumulus status. In the Fongen-Hyllingen intrusion inverted pigeonite does not appear until UZe, when the composition is more Fe-rich than En_{33} (Wilson *et al.*, 1981). Even then it only occurs rather sporadically, and it appears to co-exist with primary orthopyroxene. The precise extent of its range is not clear. The Ca-poor pyroxene phase in the Skaergaard intrusion is inverted pigeonite throughout its cumulus range (En_{62-49} approximately), but it only barely extends into UZa (Wager and Brown, 1968). Inverted pigeonite is the characteristic Ca-poor pyroxene in Bushveld UZa and UZb, with an approximate composition range of En_{60-50} (Von Gruenewaldt, 1973).

The upper zones of all four intrusions are thought to represent extreme fractionation products developed from tholeiitic basalt magma. This is clearly indicated by the pyroxene trends, by the occurrence of Fe-rich olivines, and by the eventual appearance of quartz, either as an intercumulus phase (Insch, Skaergaard, and Bushveld) or as a minor cumulus phase (Fongen-Hyllingen). It is evident from the restriction of hydrous phases (amphibole and biotite) to the intercumulus environment that the Insch intrusion crystallized under conditions of relatively low P_{H_2O} compared with Fongen-Hyllingen, where cumulus amphibole and biotite occur. Disappearance of Ca-poor pyroxene as a cumulus phase in the later fractionation stages has been interpreted as the result of increasing P_{H_2O} or increasing potassium content (Cawthorn, 1976). Although the latter explanation was favoured by Wilson *et al.* (1981) on the grounds that orthopyroxene disappeared at much the same level as cumulus alkali feldspar appeared in the Fongen-Hyllingen succession, this argument is less applicable to Insch where the incoming of cumulus alkali feldspar definitely precedes the loss of orthopyroxene.

Another aspect of the pyroxene behaviour in the Insch UZ succession appears to be unmatched elsewhere, and is not easy to explain. This is the apparent change in status of both orthopyroxene and clinopyroxene from cumulus in the MZ to intercumulus in the lower part of the UZa, and then back to cumulus higher in the same subzone and into UZb. This is indicated by their textural characteristics and by their modal scarcity in the lower part of UZa. It is not immediately clear whether their temporary absence as cumulus phases is a function of some change in physical conditions or in magma chemistry, but preliminary studies of the MZ pyroxene compositions suggest that it may be

necessary to invoke more than one pulse of magma to explain the relationships of the MZ to UZ cumulates at Insch.

More significant is the fact that the trend of pyroxene compositions seems to be independent of their cumulus or intercumulus status in UZa. This feature has been observed in other layered intrusions, such as Rhum and Kapalagulu. On Rhum, the intercumulus clinopyroxene compositions appear to follow the cumulus olivine trend early in the fractionation sequence of certain cyclic units, before clinopyroxene became established as a cumulus phase (Dunham and Wadsworth, 1978; Faithfull, 1985). At Kapalagulu, the clinopyroxene appears to fluctuate between cumulus and intercumulus habit, even though the associated orthopyroxene is consistently present as a cumulus phase (Wadsworth *et al.*, 1982). The latter type of variation can perhaps be explained in terms of minor variations in crystallization conditions, whereby periods of equilibrium precipitation of cumulus clinopyroxene were interspersed with episodes of non-equilibrium behaviour, during which nucleation of clinopyroxene was slightly delayed and was therefore restricted to the intercumulus environment, but without significant departure from equilibrium compositions. However, this type of explanation is less easily applied to the Rhum situation, since there the pyroxene composition trend in individual cyclic units is clearly established well before its first appearance as a cumulus phase. This is difficult to explain if the intercumulus magma took the same evolutionary course as the main magma, since the earliest cumulus pyroxene should be no less magnesian than its intercumulus equivalent at lower levels in the sequence.

Faithfull (1985) interpreted the Rhum pattern of variation to indicate that the present mineral compositions are not primary, and he favoured an explanation involving subsolidus Mg-Fe exchange between cumulus olivine and intercumulus clinopyroxene, so that the olivine composition trend was effectively imposed on the associated pyroxene. He preferred this explanation to one requiring re-equilibration of both phases with relatively evolved intercumulus magma, because of apparent discrepancies between the calculated Mg/Fe ratios of such magma, as indicated independently by the olivine and pyroxene compositions.

However, re-equilibration of cumulus grains with trapped intercumulus magma is likely to be a much more effective process than subsolidus reactions, and there is clear evidence that compositions have been modified in this way (e.g. Butcher, 1985). On this basis it would be possible to argue that the intercumulus material, such as the pyr-

oxene in the lower part of UZa, represents 'primary' compositions, in that it crystallized direct from the magma (albeit slightly fractionated, intercumulus magma), but that the associated cumulus phases have to some extent been 'modified' by re-equilibration with this magma. Thus, the whole assemblage might approximate to an equilibrium association, but the equilibrium represented is that of the postcumulus rather than the syncumulus stage. Such an explanation would certainly account for the smooth continuity of intercumulus and cumulus pyroxene trends, and it might also explain the rather patchy plagioclase compositions, on the grounds that complete plagioclase re-equilibration might be less easily achieved (compared with olivine or orthopyroxene, for example). Thus the most calcic plagioclase core compositions might be taken to represent the original cumulus compositions, and the more sodic parts to approximate to the new equilibrium conditions, appropriate to the early postcumulus stage of crystallization. There might also be an extension of the equilibration process into the subsolidus stage, at least in the case of structurally simpler phases such as the spinels, and there is considerable evidence that this has occurred in chromite-bearing cumulates (e.g. Henderson and Wood, 1981; Bevan, 1982).

The implications of the mechanism outlined above have not been explored in detail, and it is clear that much more information on precise composition variations within both the cumulus and intercumulus minerals is required. It might also be argued that there are so many complex factors which might influence postcumulus behaviour, such as adcumulus growth (Wadsworth, 1985), intercumulus convection (Sparks *et al.*, 1985; Tait, 1985), and infiltration metasomatism (Irvine, 1980), that any attempt to interpret cryptic variation in terms of original (or slightly modified) cumulus mineral compositions are doomed to failure. Yet the cryptic variation patterns are often surprisingly simple, as for example in the Insch Upper Zone, with the implication that postcumulus processes are less complex than recent studies imply, or that they tend to operate in a reasonably predictable and uniform fashion.

Acknowledgements. Thanks are due to Dr M. Munro (Aberdeen University) for collecting and donating samples from the temporary gas pipeline trenches, and for his general interest and encouragement in these continuing investigations of the Newer Gabbros; also to Dr J. E. Treagus (Manchester University) for logistical assistance in the field, and to Dr P. E. Champness (Manchester University) for information concerning exsolution in the Insch UZ alkali feldspars and pyroxenes.

REFERENCES

- Bevan, J. C. (1982) Reaction rims of orthopyroxene and plagioclase around chrome-spinels in olivine from Skye and Rhum (NW Scotland). *Contrib. Mineral. Petrol.* **79**, 124-9.
- Butcher, A. R. (1985) Channelled metasomatism in Rhum layered cumulates—evidence from late-stage veins. *Geol. Mag.* **122**, 503-18.
- Cawthorn, R. G. (1976) Calcium-poor pyroxene reaction relations in calc-alkaline magmas. *Am. Mineral.* **61**, 907-12.
- Clarke, P. D., and Wadsworth, W. J. (1970) The Inch layered intrusion. *Scott. J. Geol.* **6**, 7-25.
- Dunham, A. C., and Wadsworth, W. J. (1978) Cryptic variation in the Rhum layered intrusion. *Mineral. Mag.* **42**, 347-56.
- Faithfull, J. W. (1985) The Lower Eastern Layered Series of Rhum. *Geol. Mag.* **122**, 459-68.
- Henderson, P., and Wood, R. J. (1981) Reaction relationships of chrome-spinels in igneous rocks—further evidence from the layered intrusions of Rhum and Mull, Inner Hebrides, Scotland. *Contrib. Mineral. Petrol.* **78**, 225-9.
- Irvine, T. N. (1980) Magmatic infiltration metasomatism, double-diffusive fractional crystallization and adcumulus growth in the Muskox intrusion and other layered intrusions. In *Physics of Magmatic Processes* (R. B. Hargraves, ed.). Princeton University Press, 326-83.
- (1982) Terminology for layered intrusions. *J. Petrol.* **23**, 127-62.
- Read, H. H., Sadashivaiah, M. S., and Haq, B. T. (1961) Differentiation in the olivine-gabbro of the Inch mass, Aberdeenshire. *Proc. Geol. Assoc.* **72**, 391-413.
- (1965) The hypersthene-gabbro of the Inch Complex, Aberdeenshire. *Ibid.* **76**, 1-11.
- Sparks, R. S. J., Huppert, H. E., Kerr, R. C., McKenzie, D. P., and Tait, S. R. (1985) Postcumulus processes in layered intrusions. *Geol. Mag.* **122**, 555-68.
- Tait, S. R. (1985) Fluid dynamics and geochemical evolution of cyclic unit 10, Rhum, Eastern layered series. *Ibid.* **122**, 469-84.
- Von Gruenewaldt, G. (1973) The Main and Upper Zones of the Bushveld Complex in the Roossenekal area, Eastern Transvaal. *Trans. Geol. Soc. S. Africa* **76**, 207-27.
- Wadsworth, W. J. (1982) The basic plutons. In *Igneous Rocks of the British Isles* (D. Sutherland, ed.). John Wiley, 135-48.
- (1985) Terminology of postcumulus processes and products in the Rhum layered intrusion. *Geol. Mag.* **122**, 549-54.
- Dunham, A. C., and Almohandis, A. A. (1982) Cryptic variation in the Kapalagulu layered intrusion, Western Tanzania. *Mineral. Mag.* **45**, 227-36.
- Wager, L. R., and Brown, G. M. (1968) *Layered Igneous Rocks*. Oliver and Boyd, Edinburgh.
- Wilson, J. R., and Larsen, S. B. (1985) Two-dimensional study of a layered intrusion—the Hyllingen Series, Norway. *Geol. Mag.* **122**, 97-124.
- Esbensen, K. H., and Thy, P. (1981) Igneous petrology of the synorogenic Fongen-Hyllingen layered basic complex, south-central Scandinavian Caledonides. *J. Petrol.* **22**, 584-627.

APPENDIX

Analytical Methods. The mineral analyses were made using a Cambridge Instrument Company Geoscan fitted with a Link System model 290-2KX energy-dispersive spectrometer (using 15 kW, a specimen current of approximately 3 nA on cobalt metal and ZAF-4/FLS quantitative analysis software system). For olivines and orthopyroxenes the apparent composition range in each rock was generally less than 0.7% (Fo and En respectively), and for clinopyroxenes less than 1% Mg#.

[Manuscript received 6 March 1986;
revised 1 April 1986]